Tumor-reactive T cell subsets in the microenvironment of ovarian cancer

Authors:

M C W Westergaard[1], R Andersen[1,2], C Chong[5,6], JW Kjeldsen[1], M Pedersen[1,2], C Friese[1], T Hasselager[3], H Lajer[4], G. Coukos[5,6], M Bassani-Sternberg[5,6], M Donia*[1,2], I M Svane*[1,2]

Affiliations:

[1]Center for Cancer Immune Therapy, Department of Hematology, Herlev Hospital, University of Copenhagen, Denmark.

[2]Department of Oncology, Herlev Hospital, University of Copenhagen, Denmark

[3]Department of Pathology, Herlev Hospital, University of Copenhagen, Denmark

[4]Department of Gynecology, Rigshospitalet, University of Copenhagen, Denmark

[5]Ludwig Institute for Cancer Research, University of Lausanne, Switzerland

[6]Department of Oncology, University Hospital of Lausanne, Switzerland

***contributed equally to this work**

Running title:

Exploring the field of ACT for ovarian cancer

Keywords:

Ovarian cancer, tumor-infiltrating lymphocytes, cytotoxic T cells, immunopeptidomics, adoptive cell therapy

Corresponding Authors:

Inge Marie Svane, Email: inge.marie.svane@regionh.dk, phone: +4538689339, fax: +4538683457

and Marco Donia, Email: marco.donia@regionh.dk, phone: +4538681456, fax: +4538683457
Center for Cancer Immune Therapy, Department of Hematology and Department of Oncology, Herlev Hospital, University of Copenhagen, Denmark.

Abstract

Background: Solid malignancies are frequently infiltrated with T cells. The success of adoptive cell transfer (ACT) with expanded tumor-infiltrating lymphocytes (TILs) in melanoma warrant its testing in other cancer types. In this preclinical study, we investigated whether clinical-grade TILs could be manufactured from ovarian cancer (OC) tumor specimens.

Methods: 34 tumor specimens were obtained from 33 individual patients with OC. TILs were analyzed for phenotype, antigen specificity and functionality.

Results: Minimally expanded TILs (Young TILs) were successfully established from all patients. Young TILs contained a high frequency of $CD3^+$ cells with a variable CD4/CD8 ratio. TILs could be expanded to clinical numbers. Importantly, recognition of autologous tumor cells was demonstrated in TILs in >50% of the patients. We confirmed with mass-spectrometry the presentation of multiple tumor antigens, including peptides derived from the cancer-testis antigen GAGE, which could be recognized by antigen specific TILs. Antigen specific TILs could be isolated and further expanded in vitro.

Conclusion: These findings support the hypothesis that patients with OC can benefit from ACT with TILs, and led to initiation of a pilot clinical trial at our institution (clinicaltrials.gov: NCT02482090).

Introduction

The density of intratumoral infiltration with T cells has been associated with improved survival in virtually all forms of solid tumors evaluated (Zhang *et al*, 2003; Sato *et al*, 2005; Adams *et al*, 2009; Gooden *et al*, 2011). In fact, the natural infiltrates of solid tumors may contain T cells targeting several types of tumor-antigens, including those derived from tumor-specific mutated proteins (Kvistborg *et al*, 2013; Schumacher & Schreiber, 2015). A technically complex approach of personalized cancer immunotherapy based on the isolation, in vitro expansion and reinfusion of T cells isolated from the microenvironment of an individual patient's tumor metastasis has demonstrated promising results. However, so far current protocols of T cell expansion and patient conditioning have only been tested in a few selected forms of metastatic cancer (Rosenberg & Restifo, 2015).

The human immune system can naturally generate adaptive immune responses against ovarian cancer (OC) (Attig *et al*, 2009; Wick *et al*, 2014; Ye *et al*, 2014). OC has a moderately high mutational load on average (Alexandrov *et al*, 2013), and immune recognition of cancer mutations has previously been shown (Wick *et al*, 2014). Overall, OC appears to be an optimal target for strategies enhancing endogenous immune responses (Coukos *et al*, 2016).

OC is the most lethal gynecologic malignancy. It is often diagnosed at an advanced stage (e.g. International Federation of Gynecology and Obstetrics (FIGO) stage III or IV), which combined with the lack of curative medical treatment options(Armstrong *et al*, 2006), contributes to a poor relative 5 year survival rate of 39% and 17%, stage III and IV, respectively, for the most common epithelial carcinomas, which comprise 85-90% of cases (www.cancer.org, 2016). Immunotherapy

with checkpoint inhibitors have shown limited efficacy in OC so far, with response rates ranging from 6-17% (J.R. Brahmer & Tykodi, 2012; Disis *et al*, 2015; Hamanishi *et al*, 2015; Varga A *et al*, 2015). These observations prompted us to explore whether a personalized immunotherapy approach based on expansion of tumor-infiltrating lymphocytes (TILs) was feasible in patients with OC. In this study, we attempted to isolate, expand and test the antitumor activity *in vitro* of TILs obtained from a cohort of unselected patients with OC. We showed that TIL cultures can be easily generated in the laboratory, and display antitumor activities in the majority of cases. Further we demonstrate that tumor antigen-specific TILs can be isolated and expanded, with the result of increased anti-tumor response.

Patients, Materials and Methods

Patient material

We obtained 34 metastatic (intraoperative evaluation) tumor specimens from 33 individual patients with histologically verified OC. For the vast majority of the patients the cancer was in an advanced stage (Supplementary Table 1). All surgical resections were part of either a primary cytoreductive or an interval debulking procedure for OC at the Dept. of Gynaecology, Rigshospitalet, Copenhagen. From one patient, tumor specimens were received twice with 16 months interval, (total n=34 samples). Ascitic fluid was collected from 11 patients. The tumor specimens were transported to Herlev Hospital immediately after surgery, and processed within 2 hours. The scientific use of the patient material was approved by the National Committee on Health Research Ethics (protocol number H-2-2014-055).

Reagents for TILs and Tumor cells

Complete medium (CM) used for culturing TILs consisted of RPMI-1640 with GlutaMAX, 25 mM HEPES pH 7.2 (Gibco), 100 U⁄ml penicillin (Gibco), 100 lg⁄ml streptomycin (Gibco) and Fungizone® (Bristol-Myers Squibb) 1,25 µg⁄ml supplemented with 10% Human AB Serum (Sigma-Aldrich) and 6000 IU⁄ml of rhIL-2 (Proleukin, Novartis).

Rapid expansion medium (RM) used for the rapid expansion protocol (REP) consisted of AIM-V medium (Gibco) and Fungizone 1,25 µg⁄ml supplemented with 6000 IU⁄ml rhIL-2.

In addition OKT3 (anti-CD3) antibody (MACs Miltenyi Biotech), Pulmozyme (Roche), Allogeneic PBMCs (or feeder cells) obtained from buffy coats from healthy donors are used in the REP.

R10 medium used for culturing tumor cells consisted of RPMI-1640 with GlutaMAX, 25 mM HEPES pH 7.2, 100 U⁄ml penicillin, 100 µg⁄ml streptomycin and Foetal bovine serum (FBS) (Gibco). In addition Solu-Cortef (hydrocortisone sodium succinate) (the local hospital pharmacy) 500ng/ml was added to R10, the first month of establishing the tumor cell line (TCL).

Enzyme solution used for the digestion of tumor fragments consisted of RPMI-1640 with GlutaMAX, 25 mM HEPES pH 7.2, 100 U⁄ml penicillin, 100 µg⁄ml streptomycin, 1mg/mlCollagenase (Sigma-Aldrich) and 0.0125 mg/ml Pulmozyme (Genentech)

Manufacturing of TILs

Tumor tissue was isolated from the surrounding tissue and cut into 1-3 mm^3 fragments with a scalpel. Fragments were extensively washed with PBS before plating to minimize the risk of contamination of TIL cultures with peripheral blood. Tumor fragments were plated in individual wells in a 24 well culture plate with 2 ml CM. Half the media was changed three times a week. TILs were harvested when pooled TIL micro-cultures generated from 48 fragments reached a total number of $\geq 100 \times 10^6$ cells. This product, named Young TILs, had a generation time limit within 60 days. Young TILs were further expanded for 14 days in a small scale REP, as previously described

120 (Donia *et al*, 2011). Briefly, 100.000 TILs were mixed with $20x10^6$ allogenic feeder cells, OKT 3
121 antibody and master mix media containing 50% CM + 50% RM with 10% inactivated human AB
122 serum. Young TILs generated in parallel from tumor specimens of metastatic melanoma (MM)
123 were used as comparison.
124
125 Generation and validation of TCLs
126 TCLs were established either directly from tumor fragments, from media used for transportation of
127 the tumor specimens or from enzymatically digested fresh tumor fragments, named fresh tumor
128 digest (FTD). In addition, single cell suspensions of uncultured FTDs containing all cells present in
129 the tumor microenvironment (TME) were cryopreserved for later use.
130 TCLs were validated by: 1) Cytospin centrifugation of the cell suspension for morphologic
131 evaluation and 2) Formalin-fixation and paraffin-embedding (FFPE) followed by
132 immunohistochemistry (IHC) staining for various OC markers; CA125, EpCAM, PAX8, p16, p53,
133 CK7, the mesothelial cell marker Calretinin and the proliferation marker Ki67.
134 All cell lines were established internally from clinical material thus no testing for mycoplasma
135 infection was done.
136
137 Immunohistochemistry (IHC)
138 Within two hours after surgery, the tumor specimens were cut into small fragments and several
139 fragments were randomly picked for snap freeze samples in order to represent all parts of the tumor
140 tissue. 5-7 fragments were formalin fixed and embedded in paraffin before performing IHC. The
141 samples were stained for cytokeratin A for localization of the tumor tissue among stromal tissue.
142 The samples were stained for the surface immune cell markers CD45, CD4, CD8, CD20 and CD56.
143 The stained immune infiltrates were counted in 3 squares covering 0.201 mm^2 each on every slide,

using both NanoZoomer Digital Pathology (NDP.view 2) software and Fiji Image J 1.49 software. The 3 squares were placed on identical spots on every slide from the same patient with the aim to cover as much tumor tissue as possible. A consultant pathologist from Herlev Hospital supervised all the operations.

Phenotyping of TILs

Both Young TILs and rapid expanded TILs (REP-TILs) were stained using fluorochrome-labeled monoclonal antibodies (mAb; from BD bioscience, unless indicated otherwise) CD3-BV510, CD4-PerCP, CD8-BV421, CD45RA-FITC, CD45RO-PE, CCR7-PE-Cy7, CD62L-APC, CD69-PE-Cy7, CD28-APC, CD16-FITC (Dako), CD137-PE, CD56-PE-Cy7, Gamma-Delta-TCR-PE (Biolegend), LAG-3-FITC (LS Bioscience), BTLA-PE, PD-1-PE-Cy7, TIM-3-APC (eBioscience) and analyzed with a FACS canto II instrument (BD Biosciences, New Jersey, United States). The change in the phenotypic subpopulations was investigated for statistical difference using Graphpad Prism, Wilcoxon matched-pairs signed rank test.

Evaluation of Tumor reactivity

Antitumor reactivity of in vitro expanded TILs was evaluated after co-culture for 5 hours of the TILs with autologous FTDs (thawed and washed twice) or autologous TCLs pretreated with IFN-γ (100 IU/ml) or left untreated in a ratio of 3:1.Golgi plug and CD107a-BV421 were added at the beginning of incubation. Afterwards, TILs were stained for the surface markers Near-IR Live/Dead (Life Technologies), CD3-FITC, CD56-PE, CD8-QD605 (Life Technologies) and CD4-PerCP (Biolegend) and after overnight fixation and permeabilization (eBioscience) further stained for intracellular cytokines TNF-APC and IFN-γ-PE-Cy7 (all chemicals and antibody mentioned in this paragraph are from BD bioscience unless indicated otherwise). The TILs were analyzed with FACS

168 canto II (BD bioscience, New Jersey, United States). Tumor-specific TILs were defined as the
169 frequency of T cells expressing at least one of the following T cell functions: TNF, IFN-γ or
170 CD107a. A specific antitumor response was defined as the presence of minimum 0.5% responding
171 cells, with a minimum number of 50 positive events. The frequency of tumor-reactive cells in
172 stimulated samples was subtracted from unstimulated samples. 0.5% was used as a threshold for
173 detection of tumor reactivity. All TIL products were tested for tumor reactivity against FTD except
174 TILs from patient OC.TIL.03 and against autologous TCL (available from 11 patients).

175 Cytotoxicity assays

176 Standard Cr^{51} cytotox assay was performed as previously described (Donia *et al*, 2015). Briefly,
177 $5x10^5$ tumor cells (target cells) were pulsed with 20 ul Cr^{51} for 1 hour. Autologous TILs (effector
178 cells) and target cells were co-cultured for 4 h and the Cr^{51} content of the supernatants were
179 measured.

180 Results were further validated with a novel impedance based assay (xCELLigence assay) for real-
181 time detection of cytotoxicity of adherent cells (Peper *et al*, 2014). Tumor cells were added to the
182 wells, 20.000 cells per well. After 2 days, when tumor cells reached a confluent stage, TILs were
183 added with different effector:target ratios. The tumor killing was monitored in real time, with the
184 xCELLigence instrument (ACEA Bioscience, San Diego, CA, United States).

185

186 Immunopurification of HLA class-I peptides

187 Immunopurification of HLA-class-I peptides was performed on a plate format using a positive
188 pressure processor (Waters, Milford, Massachusetts), as previously described(Chong *et al*, 2018).
189 Briefly, frozen cell pellets of OC.TIL.11 ($1.6x10^8$ cells) were lysed for 1 hour at 4 °C with PBS
190 containing 0.25% sodium deoxycholate (Sigma-Aldrich), 0.2 mM iodoacetamide (Sigma-Aldrich),
191 1 mM EDTA, 1:200 Protease Inhibitors Cocktail (Sigma-Aldrich), 1 mM

192 Phenylmethylsulfonylfluoride (Roche, Basel, Switzerland), 1% octyl-beta-D glucopyranoside
193 (Sigma-Alrich). Lysates were cleared by centrifugation (Eppendorf Centrifuge, Hamburg,
194 Germany) at 4°C at maximum speed for 50 min. The plate's wells were equilibrated before the
195 addition of anti-pan HLA-I (W6/32) antibodies covalently cross-linked to Protein-A Sepharose
196 beads (Invitrogen, California, USA). The lysates were passed through the wells by gravity flow at
197 4°C. Thereafter, washes were performed with four column volumes sequentially of 150 mM, 400
198 nM and lastly again 150 mM in 20 mM Tris-HCl pH 8, using the processor. Lastly, beads were
199 washed with two column volumes of 20 mM Tris-HCl pH 8.
200 HLA-I peptides were purified with the application of a Sep-Pak tC_{18} 96-well plate (Waters). The
201 Sep-Pak plate was first conditioned with 80% acetonitrile (ACN, Merck) in 0.1 % trifluoroacetic
202 acid (TFA, Merck, Darmstadt, Switzerland) and subsequently also with 0.1% TFA. HLA complexes
203 and the bound peptides were directly eluted on to the Sep-Pak plate with 500 µL 1% TFA. C_{18} wells
204 were then washed with 0.1 % TFA before elution of HLA-I peptides with 28% ACN in 0.1% TFA.
205 Recovered HLA-I peptides were dried using vacuum centrifugation (Thermo Fisher Scientific).
206 Liquid chromatography-mass spectrometry analysis
207 Liquid chromatography-mass spectrometry (LC-MS) analysis was performed with the nanoflow
208 Ultra-HPLC Easy nLC 1200 (Thermo Fisher Scientific, LC140) coupled online to a Q Exactive HF
209 Orbitrap mass spectrometer (Thermo Fischer Scientific) with a nanoelectrospray ion source
210 (Sonation, PRSO-V1, Baden-Württemberg, Germany) as previously described(Chong *et al*, 2018).
211 Peptides were eluted over 125 min with a gradient of 0.1% FA in 80% ACN. Data was acquired
212 with data-dependent method and HCD fragmentation at normalized collision energy of 27%. The
213 MS scan range was set to 300 to 1,650 m/z with a resolution of 60,000 (200 m/z) and an AGC
214 target value of 3e6 ions. For MS/MS, AGC target values of 1e5 were used with a maximum
215 injection time of 120 ms at set resolution of 15,000 (200 *m/z*). In case of unassigned precursor

charge states, or charge states of four and above, no fragmentation was performed. The dynamic exclusion of precursor ions from further selection was set for 20 seconds.

Identification of tumor associated HLA binding peptides

We employed the MaxQuant computational proteomics platform version 1.5.5.1 to search the peak lists against the UniProt databases (Human, 42,148 entries, March 2017) and a file containing 247 frequently observed contaminants. Methionine oxidation (15.994915 Da) was set as variable modification. The second peptide identification option in Andromeda was enabled. A FDR of 0.05 and no protein FDR was set with unspecific enzyme specificity. Possible sequence matches were restricted to 8 to 25 amino acids. The initial allowed mass deviation of the precursor ion was set to 6 ppm and the maximum fragment mass deviation was set to 20 ppm. We enabled the 'match between runs' option, which allows matching of identifications same biological samples in a time window of 0.5 min and an initial alignment time window of 20 min. We extracted the 'peptides' MaxQuant output table and filtered out peptides matching to reverse and contaminants. For *in vitro* validation of immunogenicity, we selected 23 HLA peptides (Supplementary Table 2) derived from known tumor-associated proteins based on literature and tumor specificity.

Evaluation of peptide recognition

Screening for peptide recognition was carried out with IFN-γ ELISPOT assays. Briefly, nitrocellulose bottomed 96 well plates (Merck Millipore) were coated overnight at room temperature (RT) with anti-IFN-γ antibody 1-D1K (Mabtech). The plates were washed 6 times in PBS and blocked by X-vivo medium (Lonza). The TILs were added in triplicates, 100.000 cells/well. The selected peptides (Supplemental Table 2) were added at concentration 0.2 mM alongside a negative control without peptide and a positive control (SEB). After overnight incubation at 37°C and 5% CO_2, the plates were washed in PBS and IFN-γ biotinylated secondary

Ab (Mabtech) were added followed by further 2 hour incubation at RT. The plates were then again washed with PBS and Streptavidin-ALP (Mabtech) was added followed by 1 hour incubation at RT. Finally the plates were washed and enzyme substrate NBT/BCIP (Mabtech) was added. The spots were counted using the ImmunoSpot Series 2.0 Analyzer (CTL Analyzer). Background spots were subtracted from the peptide spots and an ELISPOT response was defined as more than 20 spots after background subtraction.

Anti-GAGE reactivity of *in vitro* expanded TILs was evaluated as previously described in section *Evaluation of tumor reactivity*. Though, the TILs were incubated with peptides (concentration 0.4 mM) for 7 hours. The TILs were analyzed with FACS canto II (BD bioscience, New Jersey, United States)

HLA tetramer staining and cell sorting

Tetramers coupled with PE and APC were prepared in house, as described previously (Toebes *et al*, 2006). REP-TILs were stained with CD8-PerCP, CD4-FITC (both BD bioscience), NIR and the HLA tetramer complex HLA-A3/GAGE-peptide conjugated with PE/APC. Tetramer positive cells were sorted using FACS Aria (BD bioscience, New Jersey, United States) and immediately expanded with allogeneic irradiated PBMCs, human serum and IL-2 (two consecutive REP procedures at smaller scale were carried out). In addition, GAGE specific clones were prepared by sorting one cell/well in a round bottom 96-well plate containing allogeneic irradiated PBMCs, human serum and IL-2 as described above.

Results

Processing of specimens, initial TIL outgrowth and TCL generation

Characteristics of the clinical specimens are reported in Table 1. All patients included in this study had histologically confirmed OC, the vast majority at an advanced disease stage (FIGO III or IV). Various ovarian tumor histologies were represented, including rare carcinosarcomas. Supplementary Figure 1A illustrates the distribution of histologic subtypes in this cohort (n=33).

At our center, we have considerable experience in manufacturing of TILs from MM (Donia *et al*, 2011; Andersen *et al*, 2016), head and neck cancer (Junker *et al*, 2011) and primary renal cell carcinoma (pRCC) (Andersen *et al*, 2018). In general, resected tumor specimens, from MM and pRCC, contains a well-defined area with tumor tissue which can easily be dissected from surrounding healthy tissues. In this study, all samples from OC were obtained from intraperitoneal metastases. In contrast to melanoma and pRCC, these samples were highly heterogeneous, typically more difficult to dissect precisely from surrounding healthy tissues and, in some cases, heavily infiltrated with mucinous areas (data not shown). Young TIL cultures were successfully established from all samples within 60 days (median 28 days, range [15-59]).

Autologous TCLs were established from 11 out of the 34 OC specimens, including from subtypes such as serous adenocarcinoma, carcinosarcoma and clear cell adenocarcinoma. TCLs were established with most success from transport media (7/34 cases). Establishment of TCLs from fragments and ascites were successful in 3/34 and 1/11 cases, respectively. From one patient TCLs were established from both the fragments and the transport media. The distribution of the subtypes of these TCLs is illustrated in Supplementary Figure 1B.

Massive Expansion (Rapid Expansion) of TILs

The REP is currently used in clinical trials of adoptive cell transfer (ACT) to obtain large numbers of autologous TILs for intravenous infusion.

All Young TIL cultures were further expanded with a median fold expansion of more than 1500 fold (median 1660, range [440-5544); Figure 1A). Growth kinetics and fold expansions were compared head-to-head to MM (n=11). Median fold expansion in MM-TIL appeared higher, median 2842 (range [816-6900]; p=0.09 compared to OC-TIL) however the difference was not statistically significant (Figure 1B).

Phenotype of TILs

Young TILs contained mainly $CD3^+$ cells (median 94.2%, range [77.4-98.2], Figure 2A), with a larger proportion of $CD4^+$ T cells than $CD8^+$ T cells. A low frequency of NK cells (defined as $CD3^-$ $CD56^+$ lymphocytes) was detected in most patients (median 3.3% of lymphocytes, range [0.3-18.2]; Figure 2B). In addition, we also found a small proportion of γδ T cells (median 1.5%, range [0.1-47.4] (Figure 2C).

The CD4/CD8 ratio was highly variable among all 33 individual patients (median 7.2, range [0.01-306]; Figure 2D and 2E). Most $CD4^+$ and $CD8^+$ T cells displayed a phenotype consistent with experienced Tem ($CD45RO^+CCR7^-CD62L^-$), as defined by Sallusto and Lanzavecchia (Sallusto *et al*, 2004).

REP-TILs contained almost exclusively $CD3^+$ T cells, with a slightly higher CD4/CD8 ratio (10, range [0.02-1067], p=0.07 vs Young TILs, Figure 2D). After REP, the fraction of $CD8^+$ Tem cells increased (p=0.0004) along with a reduced fraction of Naïve $CD8^+$ T cells (p<0.0001). The same pattern were observed in the $CD4^+$ T cell subpopulation Tem cells increased (p=0.0003) along with a reduced fraction of Naïve T cells (p<0.0001)) (Figure 2F, 2G).

Regarding the classic exhaustion markers a decrease in the PD-1^+ cells was observed in both the $CD8^+$ and $CD4^+$ subpopulations after REP (p=0.0002 and p<0.0001, respectively). A relative high

fraction of LAG-3$^+$ CD8$^+$ CD4$^+$ TILs were observed, Young TILs CD8$^+$ and CD4$^+$ median 88.5% range [65.5-99.3] and median 73.7% range [45.6-96.6] respectively and REP-TILs CD8$^+$ and CD4$^+$ median range and median range respectively. Meanwhile, a significant increase of the LAG-3$^+$ CD8$^+$ subpopulation after REP was observed (p=0.0263) (Figure 2H, 2I). In addition, expression of three markers, CD69, CD137 and CD28 was determined (Supplementary figure 2A and 2B).

In order to determine whether TILs were truly expanded from the TME, the characteristics of the immune infiltrates *in situ* was further analyzed and compared to expanded TILs from 5 specimens. Analysis of immune infiltrates *in situ* showed high inter-patient variations (representative examples see Supplementary Figure 3). The distribution of the 4 immune markers analyzed (CD4, CD8, CD20 and CD56) is illustrated in Supplementary Figure 4A. The distribution of the 4 immune markers was similar in FTD (Supplementary Figure 4A). The distribution of CD4$^+$ and CD8$^+$ T cells in the TME (IHC data) was compared to the distribution of the expanded CD4$^+$ and CD8$^+$ TILs from the same specimens (Supplementary Figure 4B). In TILs from each individual specimen, it appeared that similar CD4 to CD8 ratios were maintained throughout TIL expansion, with a tendency of an increase in CD4$^+$ T cells Supplementary Figure 4B). Overall, these data suggest that TILs are truly expanded from the TME of OC and not from surrounding healthy tissues.

Tumor reactivity

The antitumor activity of the in vitro expanded TILs was evaluated after co-culture of TILs and either autologous FTD or TCLs. Responses of CD8$^+$ T cells towards autologous TCLs were detected in 7 of 11 patients, median frequency in responders 1.4%, range [0.51-7.8]. Responses towards autologous TCLs pretreated with IFN-γ were detected in 5 of 11 patients, median frequency in responders 3.2%, range [2.1-8.8]. Antitumor responses of CD8$^+$ T cells to autologous

FTD was observed in 8 of 30 patients tested, median frequency in responders was 1.7%, range [0.6-3.4]. In total, $CD8^+$ T cell responses against autologous tumor cells were detected in 13 out of 31 patients tested, with a median frequency of 3.05% (considering only the highest value, when different assays were available for one individual patient) (Figure 3).

Responses of $CD4^+$ T cells to autologous TCLs were only detected when the TCL had been pretreated with IFN-γ and in this case a response of 1,6% of the $CD4^+$ T cells was only detected in 1 of 11 patients (OC.TIL.07; 9%). Three selected TCLs (OC.TIL.04, -11, -33) were analyzed for HLA-class-II expression. None of the TCL expressed HLA-class-II constitutively, but treatment with IFN-γ induced high or moderate HLA-class-II expression in one cell line (OC.TIL.33, data not shown). Antitumor responses of $CD4^+$ T cells to autologous FTD were detected in 15 of 30 patients (50%), median frequency in responders 3.3%, range [0.8-7.3]. In total, $CD4^+$ T cell responses to autologous tumor cells were detected in 16 out of 31 patients tested (52%), with a median frequency of 3.3% (considering only the highest value, when different assays were available for one individual patient) (Figure 4).

Overall, antitumor T cell responses (either $CD8^+$ or $CD4^+$ T cells) were detected in 19 of 31 patients tested (61%)

We observed a NK cell antitumor response in 8 of 29 patients. Although the median frequency of responding NK cells was generally low (1.45%), occasionally a high fraction of NK cells were recognizing autologous TCLs (Supplementary Figure 5). The NK cell antitumor responses were found in both TILs with and without an *in vitro* antitumor T cell response (data not shown).

We determined whether TILs from selected patients with OC had cytolytic activity to autologous tumors. Young TILs from patient OC.TIL.11 generated highly specific lysis of the autologous tumor cells, however, the cytotoxic potential of the TILs decreased after the TILs have been rapid expanded (Supplementary Figure 6A). Young TILs from patient OC.TIL.04 also generated specific lysis of the autologous tumor cells, whereas lysis capacity disappeared after REP (Supplementary Figure 6B). For patient OC.TIL.11, the cytolytic potential of TILs was confirmed with another assay (xCELLigence assay), where the T cell-tumor interplay can be studied in real-time for prolonged period of time. A clear correlation between the amount of effector cells per target cells and the duration of time before complete tumor elimination was observed (Supplementary Figure 6C).

Identification of immunogenic antigens presented on ovarian cancer cells.

One OC cell line (OC.TIL.11) was analyzed with LC-MS-based immunopeptidomics and multiple tumor-associated antigens were identified. The immunogenicity of these peptides was determined using IFN-γ ELISPOT assay. We identified two overlapping peptides of the GAGE cancer-testis antigen family STYYWPRPR and YYWPRPRRY eliciting a clear IFN-γ response (119 and 47 spots, respectively) in patient OC.TIL.11 (Figure 5). The responses in OC.TIL.11 were confirmed with ICS and flow cytometry analysis (Supplementary Figure 7).

GAGE specific TILs were sorted using tetramer complexes of HLA-A3/STYYWPRPR and further expanded with two consecutive REPs. This procedure resulted in one T cell culture highly enriched with GAGE-specific T cells (around 90% stained positive for the HLA-A3/STYYWPRPR-tetramer). This GAGE-specific T cell enriched culture displayed very high recognition of both the GAGE peptide STYYWPRPR and autologous TCL (Figure 6). Similar high immune recognition

was observed with one GAGE specific clone obtained from the same original TILs (Supplementary Figure 8).

Discussion

Recent successes of ACT with TILs in MM warrant investigating this treatment strategy in other cancer types. Current TIL manufacturing methods have not yet been applied to other immunogenic solid tumors such as OC.

In this study, TILs from all patients were expanded to sufficient numbers for clinical application. OC-TILs displayed growth properties similar to those of MM-TILs. We expanded TILs from MM specimens to reach ~100 x 10^9 cells (5000 fold expansion) for infusion (Donia *et al*, 2014) and clinical responses were achieved in over 40% of treated patients (Andersen *et al*, 2016).

We investigated the phenotype of the TILs before and after the REP with a broad panel of surface markers and found an abundance of effector memory T cells. This is consistent with phenotype analyses performed in other solid tumors, e.g. MM (Donia *et al*, 2011). The distribution of major T cell subpopulations, including $CD4^+$ and $CD8^+$ T cells, did not change dramatically during the REP. In general, we found a higher frequency of $CD4^+$ T cells than $CD8^+$ T cells in the expanded OC-TIL products, which was also true in the original TME. This finding differs from previous observations in the majority of melanomas (Besser *et al*, 2010). In addition we observed a relatively high expression of the exhaustion marker LAG-3 in the TILs, which could be induced by high concentration of IL-2 in the culture medium and it could be a piece in the puzzle of the low antitumor reactivity in TILs.

406

407 A recent study by the Brad Nelson group showed that OC patients receiving neoadjuvant
408 chemotherapy had tumor tissue with increased densities of $CD3^+$ and $CD8^+$ T cells compared to
409 chemotherapy-naïve tumor tissue using IHC analysis (Lo *et al*, 2016). The tumor specimens in our
410 study included 19 chemotherapy-naïve specimens and 15 specimens from patients who received
411 chemotherapy prior to the tumor resection. A preliminary analysis of these two groups did not show
412 dramatic differences in TIL expansion or phenotype (data not shown).

413

414 Current methods of TIL isolation require dissection of viable tumors from surrounding tissues. This
415 is typically achieved by scalpel separation of the tumor tissue from the healthy tissue. Our
416 experience, and macroscopic characteristics of most OC tumors, indicates that the scalpel separation
417 technique is more difficult to apply on OC tumors than MM. It is of great importance that the
418 lymphocytes are expanded from the TME and not from healthy tissue. By comparing the
419 composition of *in situ* tumor-infiltrates and expanded TILs, we provide indirect evidence that the
420 TILs in our study were truly expanded from the TME.

421

422 Most importantly, we showed that tumor-reactive TILs could be recovered from the TME in the
423 majority of patients with unselected histologies of OC. This observation resembles the findings in
424 melanoma (Dudley *et al*, 2008; Itzhaki *et al*, 2011) and other solid cancer types such as head and
425 neck squamous cell carcinoma (Junker *et al*, 2011) , metastatic gastrointestinal (GI)
426 adenocarcinomas (Turcotte *et al*, 2014), and RCC (Markel *et al*, 2009; Baldan *et al*, 2015; Andersen
427 *et al*, 2018). However, it appeared that the frequency of tumor-reactive T cells in OC-TILs was
428 lower than reported in MM-TILs (Donia *et al*, 2015). In-depth phenotypic characterization of
429 immune responses showed that tumor-reactive $CD4^+$ T cells frequently infiltrate OC. In one patient,

we confirmed direct recognition of autologous tumor cells by tumor-specific $CD4^+$ T cells. In addition, we observed significantly more $CD4^+$ T cell responses after co-culture with FTD than when using autologous TCLs. This can potentially be explained by the additional presence of antigen-presenting cells in the FTD, which can activate $CD4^+$ T cells and thereby elicit greater immune responses compared to autologous TCLs. We, and others, have previously shown that $CD4^+$ T cells can recognize autologous tumor including mutant neo-antigens, presented directly by MM tumor cells (Friedman *et al*, 2012; Linnemann *et al*, 2014; Donia *et al*, 2015). Based on these current findings, it appears that $CD4^+$ T cells also play a role in surveillance of the TME of OC.

Finally, we identified using advanced MS-based immunopeptidomics analysis tumor antigens directly presented on the tumor cells. We confirmed that two cancer-testis antigens from the GAGE family elicited T cell responses *in vitro* in one OC patient. The immunogenicity of one these peptides (YYWPRPRRY) has already been reported previously (Backer *et al*, 1999). However, for the first time to our knowledge, GAGE-specific TILs to HLA peptide STYYWPRPR were successfully isolated and expanded. This specific population displayed a profound increase in the T cell recognition of the autologous tumor cells. However, Wick et al. showed that despite successful T cell recognition of neo-antigens in OC, this may not necessarily prevent tumor progression (Wick *et al*, 2014). The same group recently showed that the expression of neo-antigens in OCs is very low compared to other cancer types. They only found a few neo-antigen-specific $CD4^+$ and $CD8^+$ T cell responses *in vitro* and none *in vivo* using neo-antigen-specific vaccines. OC is mostly driven by large-scale mutations, and current bioinformatic prediction tools may not be able to predict which neo-antigens are presented in OC (Martin *et al*, 2016). Additional methods, such as LC-MS-based immunopeptidomics, may provide additional insights into the antigen repertoire of OC (Bassani-Sternberg & Coukos, 2016).

In conclusion, we showed that TILs could efficiently be expanded from OC. However, unselected TILs from OC generally contain small amounts of tumor-reactive T cells. One of the limiting factors could be the ability to enrich for tumor-reactive T cells, which could be achieved using novel technologies (Ye *et al*, 2014; Kelderman *et al*, 2016). These data encourage further studies to test the efficacy of ACT in OC and highlight the need for improved methods of manufacturing to increase the quality of TIL products.

Additional Information

Ethics approval

The Danish National Committee on Health Research Ethics approved the scientific use of the patient material (protocol number H-2-2014-055).

Conflicts of Interest Disclosure

The authors declare no conflicts of interest

Funding

The studies were supported by grants from the OvaCure Foundation, the Danish Cancer Society Research Foundation, the Anticancer Fund and Aase og Ejnar Danielsens Foundation.

Authors' contributions

MCWW conceived and designed experiments, developed methodology, acquired data, analyzed and interpreted data, and wrote the manuscript.

CC acquired data, analyzed and interpreted data, and wrote the manuscript.

RA, JWK, MP and CF acquired data and proof-read the manuscript.

TH and HL acquired data, analyzed and interpreted data, and wrote the manuscript.

GC, MBS, MD and IMS supervised the study.

Acknowledgements

Lissen Ingvartsen is acknowledged for assistance in patient inclusion.

References

Adams SF, Levine DA, Cadungog MG, Hammond R, Facciabene A, Olvera N *et al.* (2009) Intraepithelial T cells and tumor proliferation: Impact on the benefit from surgical cytoreduction in advanced serous ovarian cancer. *Cancer* **115**: 2891–2902, doi:10.1002/cncr.24317.

Alexandrov LB, Nik-Zainal S, Wedge DC, Aparicio S a JR, Behjati S, Biankin A V *et al.* (2013) Signatures of mutational processes in human cancer. *Nature* **500**: 415–421, doi:10.1038/nature12477.

Andersen R, Donia M, Ellebæk E, Borch TH, Kongsted P, Iversen TZ *et al.* (2016) Long-Lasting Complete Responses in Patients with Metastatic Melanoma after Adoptive Cell Therapy with Tumor-Infiltrating Lymphocytes and an Attenuated IL2 Regimen. *Clin Cancer Res* **22**: doi:10.1158/1078-0432.CCR-15-1879.

Andersen R, Westergaard MCW, Kjeldsen JW, Muller A, Pedersen NW, Hadrup SR *et al.* (2018) T-cell responses in the microenvironment of primary renal cell carcinoma-implications for adoptive cell therapy. *Cancer Immunol Res* **6**: doi:10.1158/2326-6066.CIR-17-0467.

Armstrong DK, Bundy B, Wenzel L, Huang HQ, Baergen R, Lele S *et al.* (2006) Intraperitoneal cisplatin and paclitaxel in ovarian cancer. *N Engl J Med* **354**: 34–43, doi:10.1097/01.ogx.0000206353.22975.c5.

Attig S, Hennenlotter J, Pawelec G, Klein G, Koch SD, Pircher H *et al.* (2009) Simultaneous infiltration of polyfunctional effector and suppressor T cells into renal cell carcinomas. *Cancer Res* **69**: 8412–8419, doi:10.1158/0008-5472.CAN-09-0852.

Backer O De, Arden KC, Boretti M, Smet C De, Czekay S, Viars CS *et al.* (1999) Characterization of the GAGE Genes That Are Expressed in Various Human Cancers and in Normal Testis Characterization of the GAGE Genes That Are Expressed in Various Human Cancers and in Normal Testis 1. *Cancer Res* **59**: 3157–3165.

508 Baldan V, Griffiths R, Hawkins RE, Gilham DE (2015) Efficient and reproducible generation of
509 tumour-infiltrating lymphocytes for renal cell carcinoma. *Br J Cancer* 1–9,
510 doi:10.1038/bjc.2015.96.
511 Bassani-Sternberg M, Coukos G (2016) Mass spectrometry-based antigen discovery for cancer
512 immunotherapy. *Curr Opin Immunol* **41**: 9–17, doi:10.1016/j.coi.2016.04.005.
513 Besser MJ, Shapira-Frommer R, Treves AJ, Zippel D, Itzhaki O, Hershkovitz L *et al.* (2010)
514 Clinical responses in a phase II study using adoptive transfer of short-term cultured tumor
515 infiltration lymphocytes in metastatic melanoma patients. *Clin Cancer Res* **16**: 2646–2655,
516 doi:10.1158/1078-0432.CCR-10-0041.
517 Chong C, Marino F, Pak H, Racle J, Daniel RT, Müller M *et al.* (2018) High-throughput and
518 Sensitive Immunopeptidomics Platform Reveals Profound Interferonγ-Mediated Remodeling of the
519 Human Leukocyte Antigen (HLA) Ligandome. *Mol Cell Proteomics* **17**: 533–548,
520 doi:10.1074/mcp.TIR117.000383.
521 Coukos G, Tanyi J, Kandalaft LE (2016) Opportunities in immunotherapy of ovarian cancer. *Ann*
522 *Oncol* **27**: i11–i15, doi:10.1093/annonc/mdw084.
523 Disis ML, Patel M, Pant S, Hamilton EP, Lockhart AC, Kelly K, Thaddeus-Beck J *et al.* (2015)
524 2749 Avelumab (MSB0010718C), an anti-PD-L1 antibody, in patients with recurrent or refractory
525 ovarian cancer: A phase Ib trial reporting safety and clinical activity. *Eur J Cancer* **51**: S546–S547,
526 doi:10.1016/S0959-8049(16)31515-5.
527 Donia M, Junker N, Ellebaek E, Andersen MH, Straten PT, Svane IM (2011) Characterization and
528 comparison of 'standard' and 'young' tumour-infiltrating lymphocytes for adoptive cell therapy at a
529 danish translational research institution. *Scand J Immunol* **75**: 157–167, doi:10.1111/j.1365-
530 3083.2011.02640.x.
531 Donia M, Larsen SM, Met O, Svane IM (2014) Simplified protocol for clinical-grade tumor-

532 infiltrating lymphocyte manufacturing with use of the Wave bioreactor. *Cytotherapy*
533 doi:10.1016/j.jcyt.2014.02.004.
534 Donia M, Andersen R, Kjeldsen JW, Fagone P, Munir S, Nicoletti F *et al.* (2015) Aberrant
535 expression of MHC Class II in melanoma attracts inflammatory tumor specific CD4+ T cells which
536 dampen CD8+ T cell antitumor reactivity. *Cancer Res* **75**: 3747–3760, doi:10.1158/0008-
537 5472.CAN-14-2956.
538 Dudley ME, Wunderlich JR, Shelton TE, Even J, Rosenberg SA (2008) Generation of tumor-
539 infiltrating lymphocyte cultures for use in adoptive transfer therapy for melanoma patients. *J*
540 *Immunother* **26**: 332–342, doi:10.1097/00002371-200307000-00005.
541 Friedman KM, Prieto PA, Devillier LE, Gross CA, Yang JC, Wunderlich JR *et al.* (2012) Tumor-
542 specific CD4+ Melanoma Tumor-infiltrating Lymphocytes. *J Immunother* **35**: 400–408,
543 doi:10.1097/CJI.0b013e31825898c5.
544 Gooden MJM, de Bock GH, Leffers N, Daemen T, Nijman HW (2011) The prognostic influence of
545 tumour-infiltrating lymphocytes in cancer: a systematic review with meta-analysis. *Br J Cancer*
546 **105**: 93–103, doi:10.1038/bjc.2011.189.
547 Hamanishi J, Mandai M, Ikeda T, Minami M, Kawaguchi A, Murayama T *et al.* (2015) Safety and
548 Antitumor Activity of Anti-PD-1 Antibody, Nivolumab, in Patients With Platinum-Resistant
549 Ovarian Cancer. *J Clin Oncol* doi:10.1200/JCO.2015.62.3397.
550 Itzhaki O, Hovav E, Ziporen Y, Levy D, Kubi A, Zikich D *et al.* (2011) Establishment and large-
551 scale expansion of minimally cultured 'young' tumor infiltrating lymphocytes for adoptive transfer
552 therapy. *J Immunother* **34**: 212–220, doi:10.1097/CJI.0b013e318209c94c.
553 J.R. Brahmer, Tykodi (2012) Safety and activity of anti-PD-L1 antibody in patients with advanced
554 cancer. *N Engl J Med* **188**: 2148–2149, doi:10.1016/j.juro.2012.08.169.
555 Junker N, Andersen MH, Wenandy L, Dombernowsky SL, Kiss K, Sørensen CH *et al.* (2011)

Bimodal ex vivo expansion of T cells from patients with head and neck squamous cell carcinoma: a prerequisite for adoptive cell transfer. *Cytotherapy* **13**: 822–834, doi:10.3109/14653249.2011.563291.

Kelderman S, Heemskerk B, Fanchi L, Philips D, Toebes M, Kvistborg P *et al.* (2016) Antigen-specific TIL therapy for melanoma: A flexible platform for personalized cancer immunotherapy. *Eur J Immunol* **46**: 1351–1360, doi:10.1002/eji.201545849.

Kvistborg P, van Buuren MM, Schumacher TN (2013) Human cancer regression antigens. *Curr Opin Immunol* **25**: 284–290, doi:10.1016/j.coi.2013.03.005.

Linnemann C, Buuren MM Van, Bies L, Verdegaal EME, Schotte R, Calis JJ a, Behjati S *et al.* (2014) High-throughput epitope discovery reveals frequent recognition of neo-antigens by CD4 + T cells in human melanoma. *Nat Med* **21**: 1–7, doi:10.1038/nm.3773.

Lo CS, Sanii S, Kroeger DR, Milne K, Talhouk A, Chiu DS *et al.* (2016) Neoadjuvant chemotherapy of ovarian cancer results in three patterns of tumor-infiltrating lymphocyte response with distinct implications for immunotherapy. *Am Assoc Cancer Res* clincanres.1433.2016, doi:10.1158/1078-0432.ccr-16-1433.

Markel GAL, Cohen-sinai T, Besser MJ, Oved K, Itzhaki O, Seidman R *et al.* (2009) Preclinical Evaluation of Adoptive Cell Therapy for Patients with Metastatic Renal Cell Carcinoma. **154**: 145–154.

Martin SD, Brown SD, Wick DA, Nielsen JS, Kroeger DR, Twumasi-Boateng K *et al.* (2016) Low mutation burden in ovarian cancer may limit the utility of neoantigen-targeted vaccines. *PLoS One* **11**: 1–22, doi:10.1371/journal.pone.0155189.

Peper JK, Schuster H, Löffler MW, Schmid-Horch B, Rammensee H-G, Stevanović S (2014) An impedance-based cytotoxicity assay for real-time and label-free assessment of T-cell-mediated killing of adherent cells. *J Immunol Methods* **405**: 192–198, doi:10.1016/j.jim.2014.01.012.

Rosenberg SA, Restifo NP (2015) Adoptive cell transfer as personalized immunotherapy for human cancer. *Science (80-)* **348**: 62–68, doi:10.1126/science.aaa4967.

Sallusto F, Geginat J, Lanzavecchia A (2004) Central memory and effector memory T cell subsets: function, generation, and maintenance. *Annu Rev Immunol* **22**: 745–763, doi:10.1146/annurev.immunol.22.012703.104702.

Sato E, Olson SH, Ahn J, Bundy B, Nishikawa H, Qian F *et al.* (2005) Intraepithelial CD8+ tumor-infiltrating lymphocytes and a high CD8+/regulatory T cell ratio are associated with favorable prognosis in ovarian cancer. *Proc Natl Acad Sci U S A* **102**: 18538–18543, doi:10.1073/pnas.0509182102.

Schumacher TN, Schreiber RD (2015) Neoantigens in cancer immunotherapy. *Science* **348**: 69–74, doi:10.1126/science.aaa4971.

Toebes M, Coccoris M, Bins A, Rodenko B, Gomez R, Nieuwkoop NJ *et al.* (2006) Design and use of conditional MHC class I ligands. *Nat Med* **12**: 246–251, doi:10.1038/nm1360.

Turcotte S, Gros A, Tran E, Lee CCR, Wunderlich JR, Robbins PF *et al.* (2014) Tumor-Reactive cd8+ tcells in metastatic gastrointestinal cancer refractory to chemotherapy. *Clin Cancer Res* **20**: 331–343, doi:10.1158/1078-0432.CCR-13-1736.

Varga A, Piha-Paul SA, Ott PA, Mehnert JM, Berton-Rigaud D, Johnson EA *et al.* (2015) Antitumor activity and safety of pembrolizumab in patients (pts) with PD-L1 positive advanced ovarian cancer: Interim results from a phase Ib study. *J Clin Oncol* **33(Suppl.)**: (suppl; abstr 5510).

Wick D a, Webb JR, Nielsen JS, Martin SD, Kroeger DR, Milne K *et al.* (2014) Surveillance of the tumor mutanome by T cells during progression from primary to recurrent ovarian cancer. *Clin Cancer Res* **20**: 1125–1134, doi:10.1158/1078-0432.CCR-13-2147.

www.cancer.org (2016) http://www.cancer.org/cancer/ovariancancer/detailedguide/ovarian-cancer-survival-rates.

Ye Q, Song D-G, Poussin M, Yamamoto T, Best A, Li C *et al.* (2014) CD137 Accurately Identifies and Enriches for Naturally Occurring Tumor-Reactive T Cells in Tumor. *Clin cancer Res* **20**: 44–55, doi:10.1158/1078-0432.CCR-13-0945.

Zhang L, Conejo-Garcia JR, Katsaros D, Gimotty P a, Massobrio M, Regnani G *et al.* (2003) Intratumoral T cells, recurrence, and survival in epithelial ovarian cancer. *N Engl J Med* **348**: 203–213, doi:10.1056/NEJMoa020177.

Figure 1: Ovarian Tumor infiltrating lymphocytes (TILs).

Young TILs were further expanded using a small scale Rapid Expansion Protocol (REP) **(A)** Fold expansion of TILs from 24 ovarian cancer (OC) patients (purple lines) and from 11 metastatic melanoma (MM) patients (blue lines) following a 14 days REP performed in parallel were compared. Median fold expansion for all OC patients (n=34) was 1660 (range [440-5544]). Median fold expansion for MM (n=11) was 2842 (range [816-6900]). **(B)** Scatterplot showing the final fold expansion. No significant difference was seen when comparing the final fold expansion of OC-TILs (n=34) and MM-TILs (n=11). The two groups were compared using Mann-Whitney test. Data are presented with median.

Figure 2: Phenotypic characterization of ovarian cancer TILs.

Young TILs and REP TILs were analyzed with flow cytometry for phenotypic markers **(A)** Scatterplot showing percentages of $CD3^+$ T cells in Young TIL(n=34) and REP TIL (n=33) populations. Data are presented with median. **(B)** Scatterplot showing the percentage of NK cells in the Young TIL population (n=34). Data are presented with median. **(C)** Scatterplot showing percentages of γδ T cells in Young TIL (n=34) and REP TIL(n=33) populations. Data are presented with median. **(D)** Scatterplot showing the CD4/CD8 ratios in Young TILs (n=34) and REP TILs (n=33). The median CD4/CD8 ratio in Young TILs was 7.2 (range [0.01-306]) and 10.0 (range [0.02-1067]) in REP TIL population. Data were log transformed before the two groups were compared. A significant increase of the ratio was observed (p=0.0253). Data are presented with median. **(E)** The pie charts show the phenotypic distribution of $CD8^+$, $CD4^+$, $CD4^+CD8^+$ and $CD4^-$ $CD8^-$ of $CD3^+$ TILs in the Young TIL (n=34) and REP TIL (n=33) populations. Data are presented with mean values.

(F and G) scatterplots illustrating the percentage of naïve T cells, central memory T cells and effector memory T cells and **(H and I)** scatterplots illustrating the percentage of Exhaustion markers; LAG-3, BTLA, PD-1 and TIM-3 in **(F and H)** the $CD8^+$ T cell population and **(G and I)** the $CD4^+$ T cell population in Young TILs (n=34) and REP TILs (n=33). Data are presented with median with interquartile range.

(F) Shows significant increase of $CD8^+$ Tem cells p=0.0004 during the REP and a significant decrease in the Naïve T cell subpopulation, p<0.0001. **(G)** The CD4 expressing population had a significant increase in $CD4^+$ Tem cells during the REP, p=0.0003, and a significant decrease in the Naïve T cell subpopulation during the REP, p<0.0001.

(H) Shows significant increase of $CD8^+$ $LAG\text{-}3^+$ T cells p=0.0263 during the REP and a significant decrease in the $PD\text{-}1^+$ T cells, p=0.0002, and a significant increase in the $TIM\text{-}3^+$ T cells, p=0.0379 **(I)** The CD4 expressing population had a significant decrease in $CD4^+$ $BTLA^+$ cells during the REP, p=0.013, and a significant decrease in the $PD\text{-}1^+$ T cell subpopulation during the REP, p<0.0001.

Young TILs and REP TILs were compared using Wilcoxon signed rank test. Statistical significant differences is indicated with *, **, *** or **** for p-values less than 0.05, 0.01, 0.001, or 0.0001 respectively.

Figure 3: In vitro anti-tumor activity of $CD8^+$ Young TILs.

The antitumor activity of the in vitro expanded TILs was evaluated by defining the frequency of T cells expressing at least one of the following T cell functions: TNF, IFN-γ or CD107a, upon stimulation with autologous Fresh tumor digest (FTD) or tumor cell line (TCL) treated with low-dose IFN-γ (100 IU/ml) or left untreated. A specific anti-tumor response was defined as the presence of minimum 0.5% responding cells, with a minimum number of 50 positive events. The frequency of tumor-reactive cells in stimulated samples was subtracted from un-stimulated

samples. 0.5% was used as a threshold for detection of tumor reactivity. **(A)** Antitumor-responses of $CD8^+$ T cells were detected in **13 of 31 patients** analyzed. *: OC.TIL.03 is not tested with FTD. ϕ: TILs generated from OC.TIL.04 2^{nd} was tested for reactivity against FTD from OC.TIL.04 **(B)**. FACS plot showing cytokine production from TIL alone (unstimulated, serving as a negative control) and TIL stimulated with autologous TCL, from a representative patient. **(C)** FACS plot showing CD107a mobilization of TIL upon co-culture with an autologous TCL. Unstimulated TIL (TIL alone) serves as a negative control.

Figure 4: In vitro anti-tumor activity of $CD4^+$ Young TILs.

The antitumor activity of the in vitro expanded TILs was evaluated by defining the frequency of T cells expressing at least one of the following T cell functions: TNF, IFN-γ or CD107a, upon stimulation with autologous Fresh tumor digest (FTD) or tumor cell line (TCL) treated with low-dose IFN-γ (100 IU/ml) or left untreated. A specific anti-tumor response was defined as the presence of minimum 0.5% responding cells, with a minimum number of 50 positive events. The frequency of tumor-reactive cells in stimulated samples was subtracted from un-stimulated samples0.5% was used as a threshold for detection of tumor reactivity. **(A)** Antitumor-responses of CD4+ T cells were detected in **16 of 31 patients**. *OC.TIL.03 is not tested with FTD. ϕ: TILs generated from OC.TIL.04 2^{nd} was tested for reactivity against FTD from OC.TIL.04. **(B)** FACS plot showing cytokine production from TIL alone (unstimulated, serving as a negative control) and TIL stimulated with autologous TCL, from a representative patient.

Figure 5: IFN-γ ELISPOT assay: Selected peptides identified by MS-based immunopeptidomics tested for ability to induce a IFN-γ response in REP TILs from patient OC.TIL.11. Background

(spots in wells without added peptides) was subtracted. Example of IFN- γ ELISPOT response against GAGE peptides.

Figure 6: GAGE specific TILs.

(A) 1600 GAGE12 specific Young TILs from patient OC.TIL.11 were sorted using tetramers HLA-A3/ STYYWPRPR APC/PE. **(B)** The sorted culture was tested for specificity with tetramers HLA-A3/ STYYWPRPR APC/PE after 2 times REP.

(C) FACS plot illustrating cytokine production (upper panel) and CD107a mobilization (lower panel) in TIL alone (unstimulated) as a negative control, TILs stimulated with autologous tumor cell line (TCL), TILs stimulated with autologous TCL pre-stimulated with IFN-γ for 3 days prior to experiment and TILs stimulated with the GAGE peptide.

A

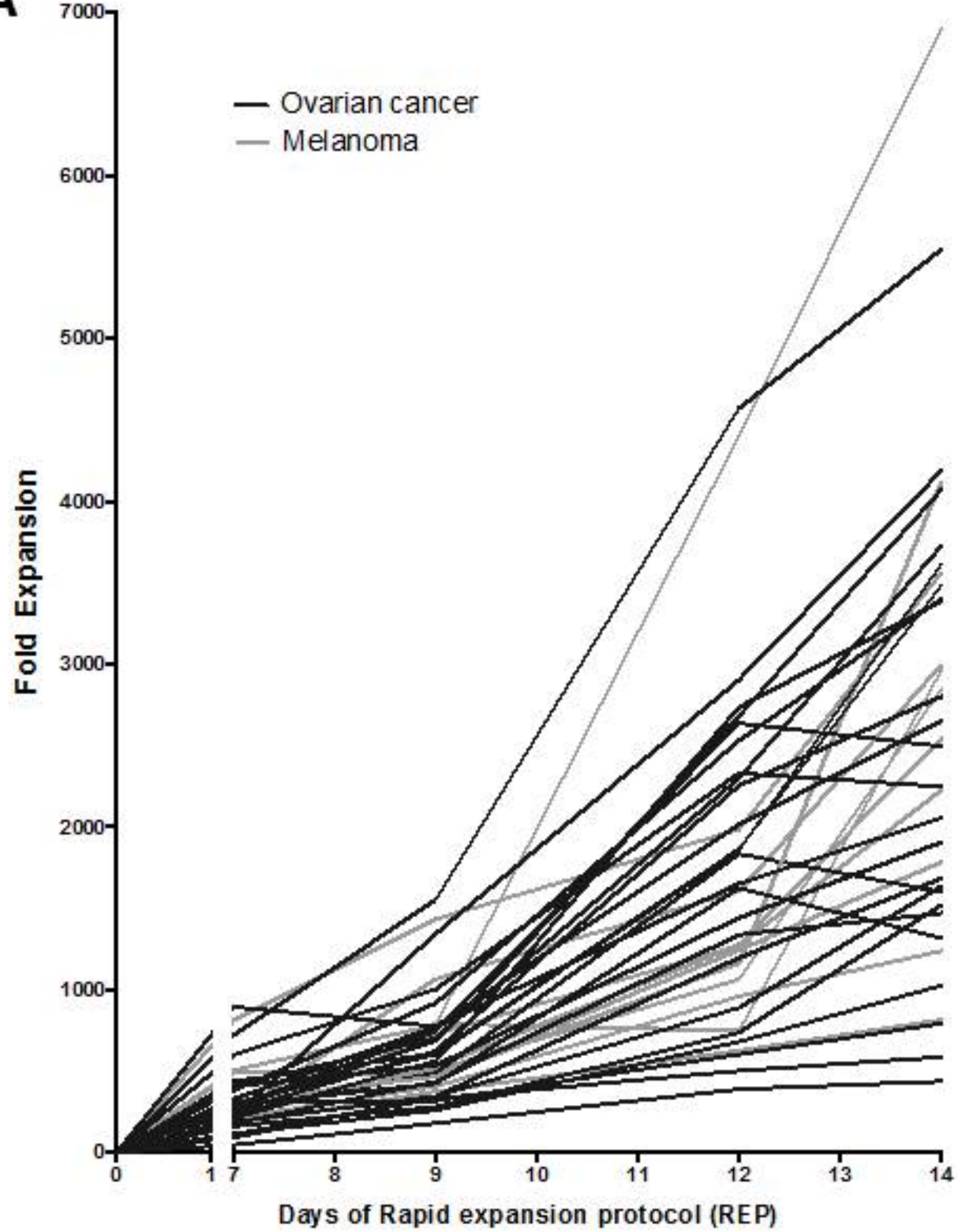
Ovarian cancer
Melanoma
Fold Expansion
7000
6000
5000
4000
3000
2000
1000
0
0
1
7
8
9
10
11
12
13
14
Days of Rapid expansion protocol (REP)

B

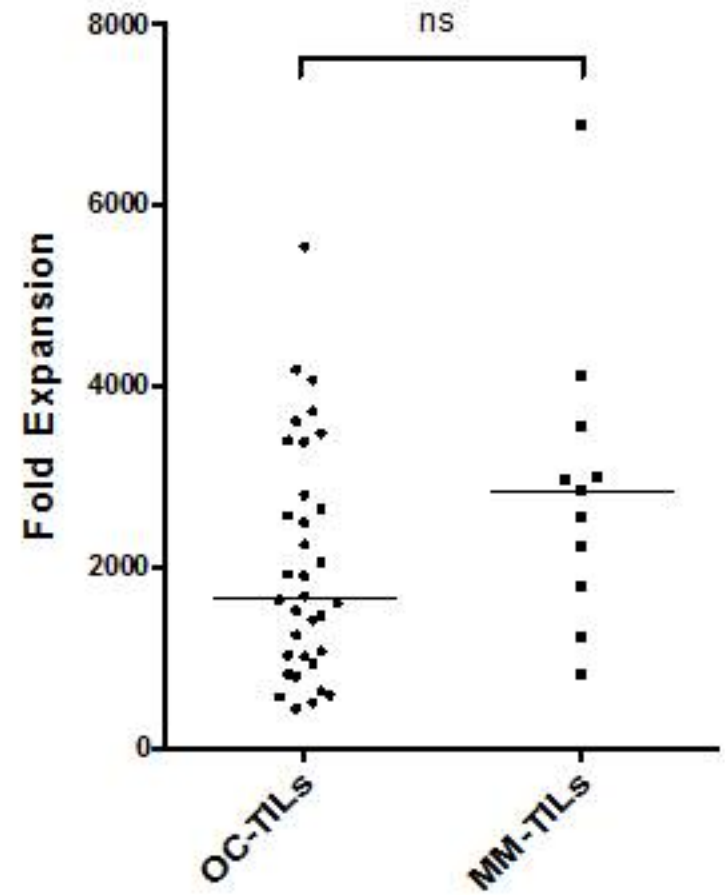
ns
Fold Expansion
8000
6000
4000
2000
0
OC-TILs
MM-TILs

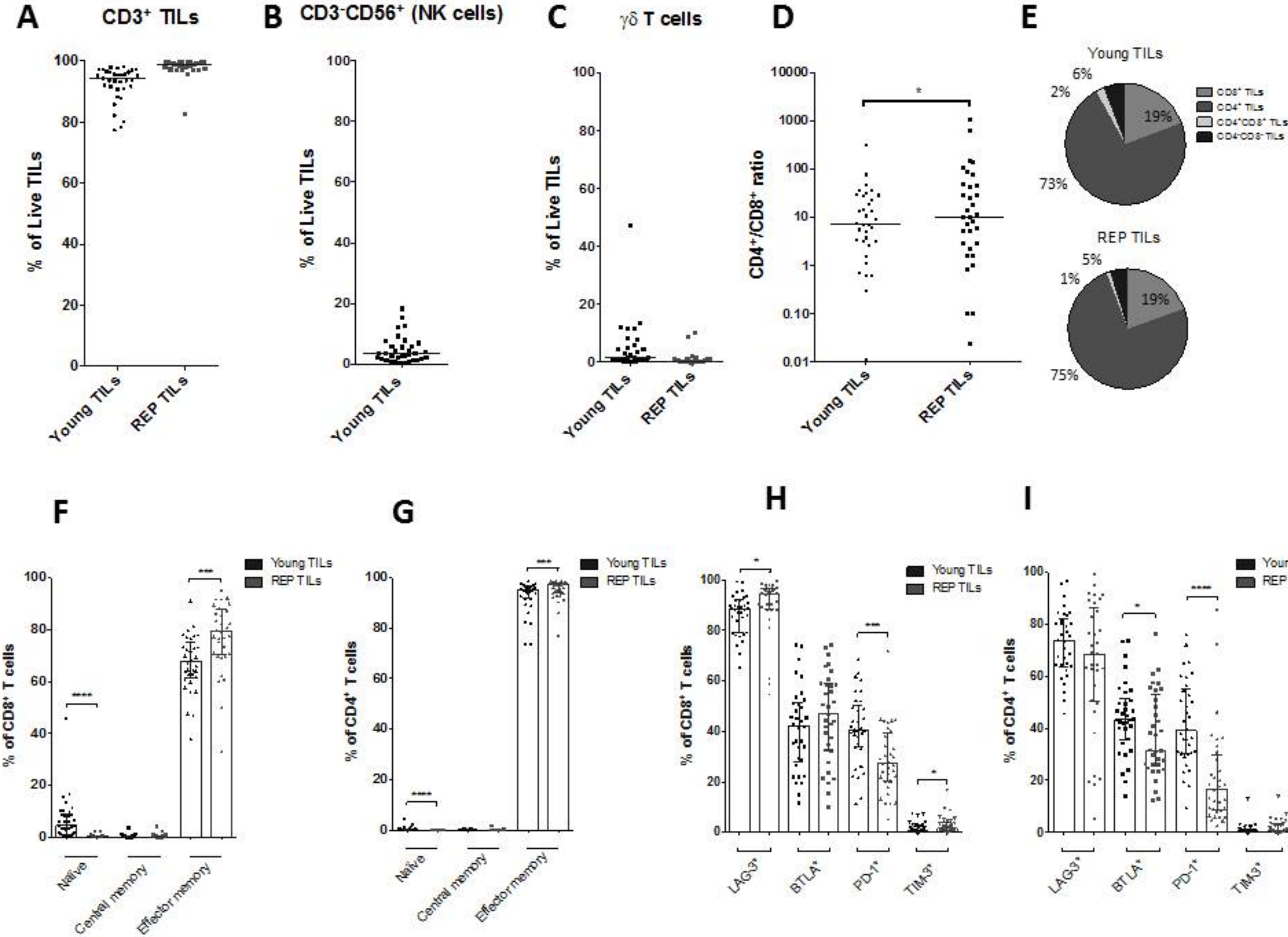
A
CD3+ TILs
% of Live TILs
Young TILs
REP TILs
B
CD3-CD56+ (NK cells)
% of Live TILs
Young TILs
C
γδ T cells
% of Live TILs
Young TILs
REP TILs
D
CD4+/CD8+ ratio
*
Young TILs
REP TILs
E
Young TILs
6%
2%
19%
73%
CD8+ TILs
CD4+ TILs
CD4+CD8+ TILs
CD4-CD8- TILs
REP TILs
5%
1%
19%
75%
F
Young TILs
REP TILs
% of CD8+ T cells
Naïve
Central memory
Effector memory
G
Young TILs
REP TILs
% of CD4+ T cells
Naïve
Central memory
Effector memory
H
Young TILs
REP TILs
% of CD8+ T cells
LAG3+
BTLA+
PD-1+
TIM3+
I
Young TI
REP TILs
% of CD4+ T cells
LAG3+
BTLA+
PD-1+
TIM3+

A

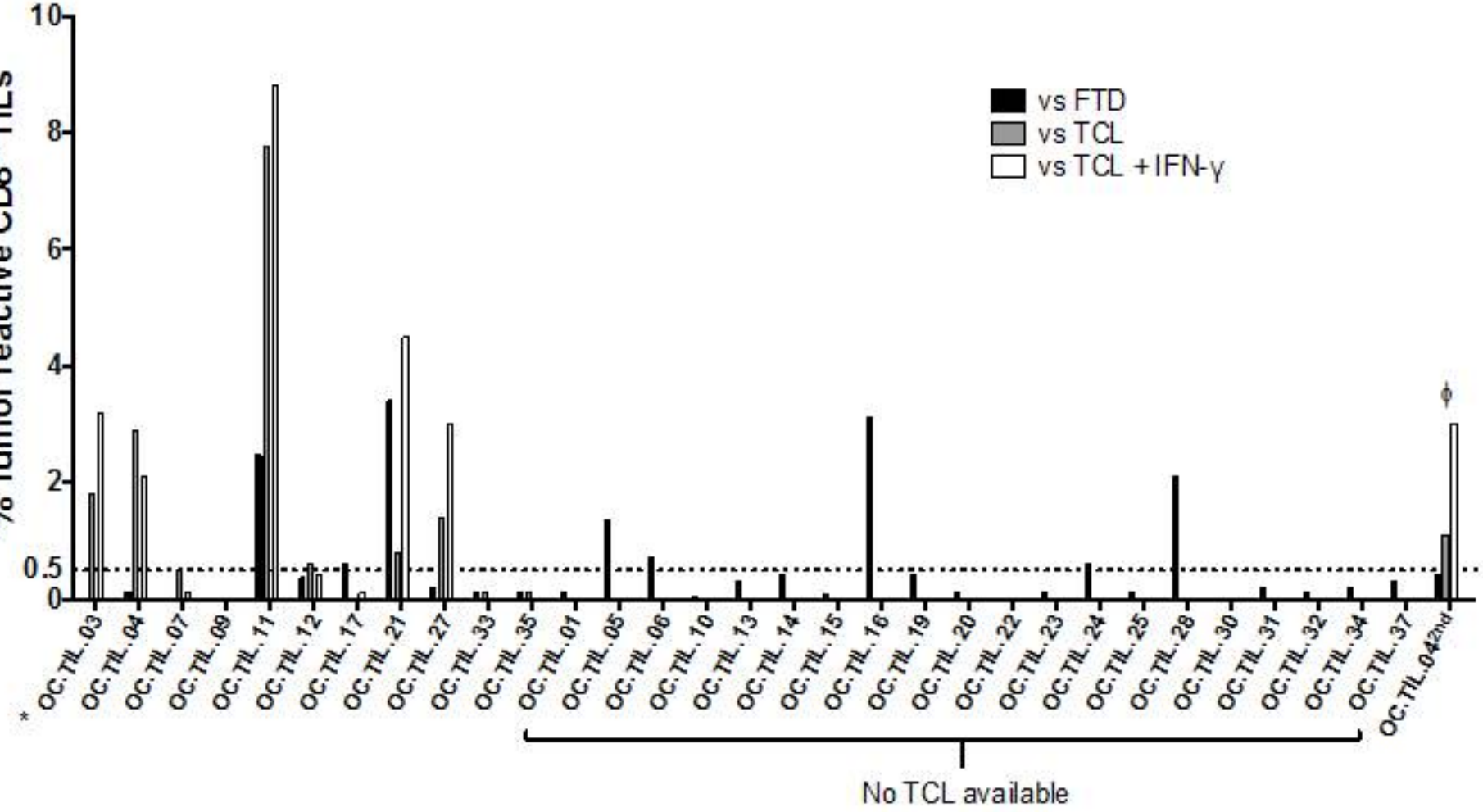
% Tumor reactive CD8+ TILs
10
8
6
4
2
0.5
0
vs FTD
vs TCL
vs TCL +IFN-γ
ϕ
OC.TIL.03
OC.TIL.04
OC.TIL.07
OC.TIL.09
OC.TIL.11
OC.TIL.12
OC.TIL.17
OC.TIL.21
OC.TIL.27
OC.TIL.33
OC.TIL.35
OC.TIL.01
OC.TIL.05
OC.TIL.06
OC.TIL.10
OC.TIL.13
OC.TIL.14
OC.TIL.15
OC.TIL.16
OC.TIL.19
OC.TIL.20
OC.TIL.22
OC.TIL.23
OC.TIL.24
OC.TIL.25
OC.TIL.28
OC.TIL.30
OC.TIL.31
OC.TIL.32
OC.TIL.34
OC.TIL.37
OC.TIL.042nd
*
No TCL available

B

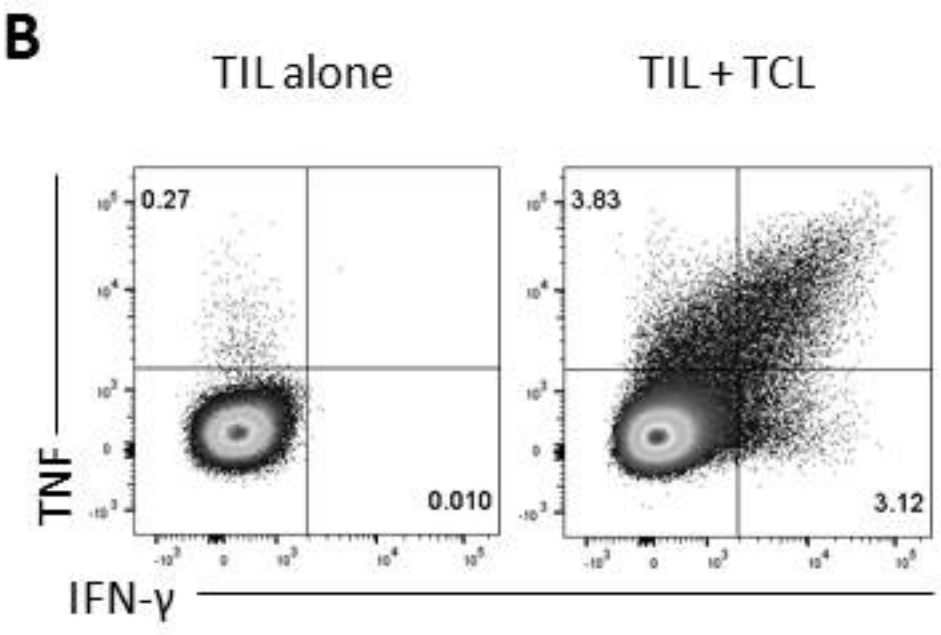
TIL alone
TIL + TCL
0.27
0.010
3.83
3.12
TNF
IFN-γ

C

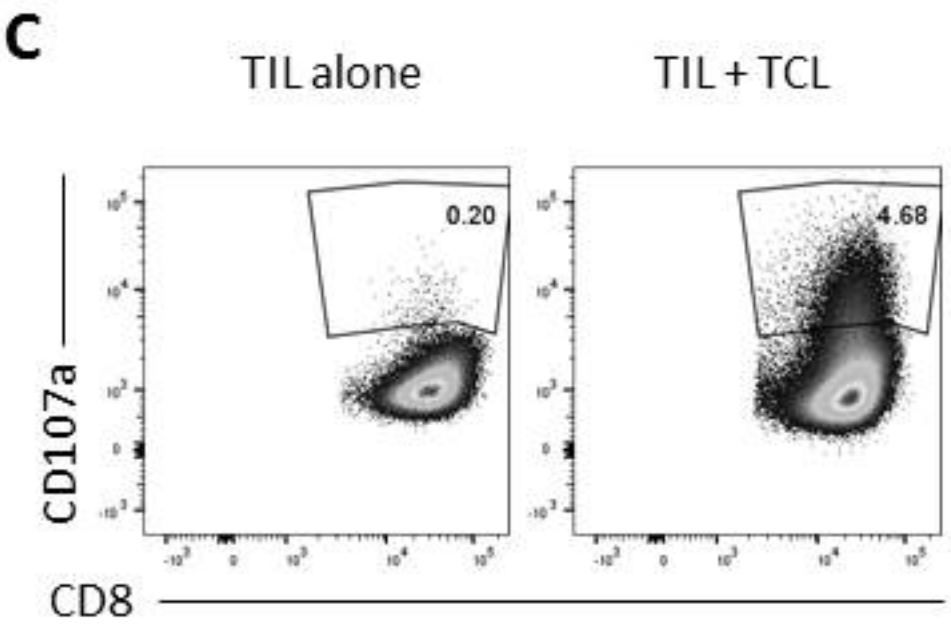
TIL alone
TIL + TCL
0.20
4.68
CD107a
CD8

A

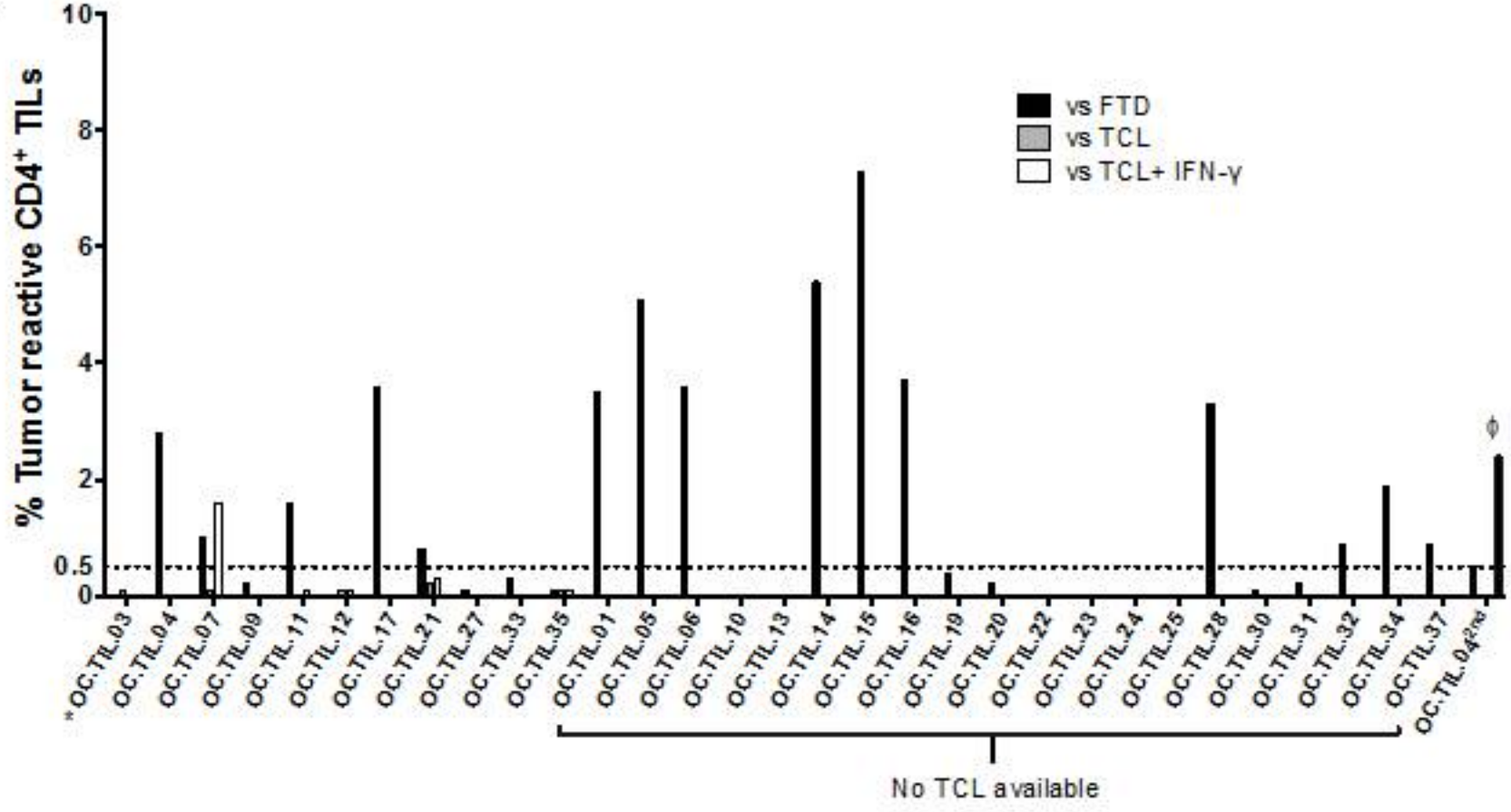
% Tumor reactive CD4+ TILs
10
8
6
4
2
0.5
0
vs FTD
vs TCL
vs TCL+ IFN-γ
ϕ
*OC.TIL.03
OC.TIL.04
OC.TIL.07
OC.TIL.09
OC.TIL.11
OC.TIL.12
OC.TIL.17
OC.TIL.21
OC.TIL.27
OC.TIL.33
OC.TIL.35
OC.TIL.01
OC.TIL.05
OC.TIL.06
OC.TIL.10
OC.TIL.13
OC.TIL.14
OC.TIL.15
OC.TIL.16
OC.TIL.19
OC.TIL.20
OC.TIL.22
OC.TIL.23
OC.TIL.24
OC.TIL.25
OC.TIL.28
OC.TIL.30
OC.TIL.31
OC.TIL.32
OC.TIL.34
OC.TIL.37
OC.TIL.04 2nd
No TCL available

B

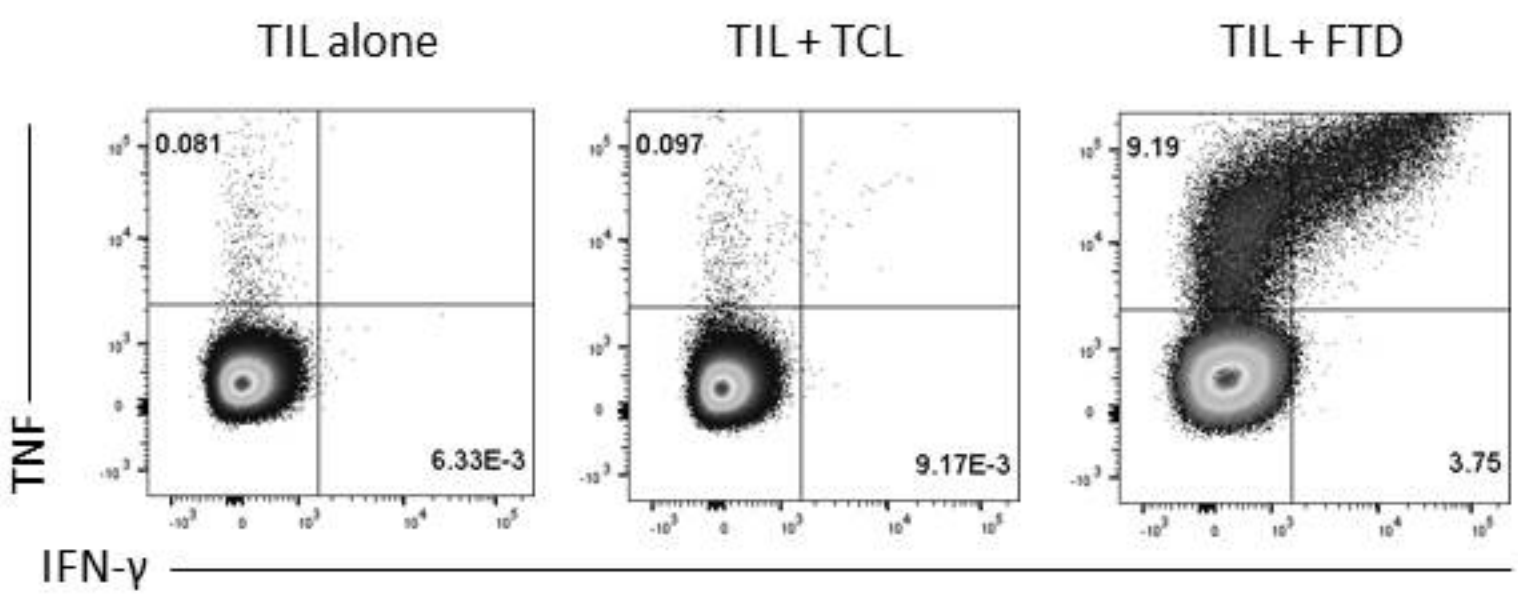
TIL alone
TIL + TCL
TIL + FTD
0.081
6.33E-3
0.097
9.17E-3
9.19
3.75
TNF
IFN-γ

A

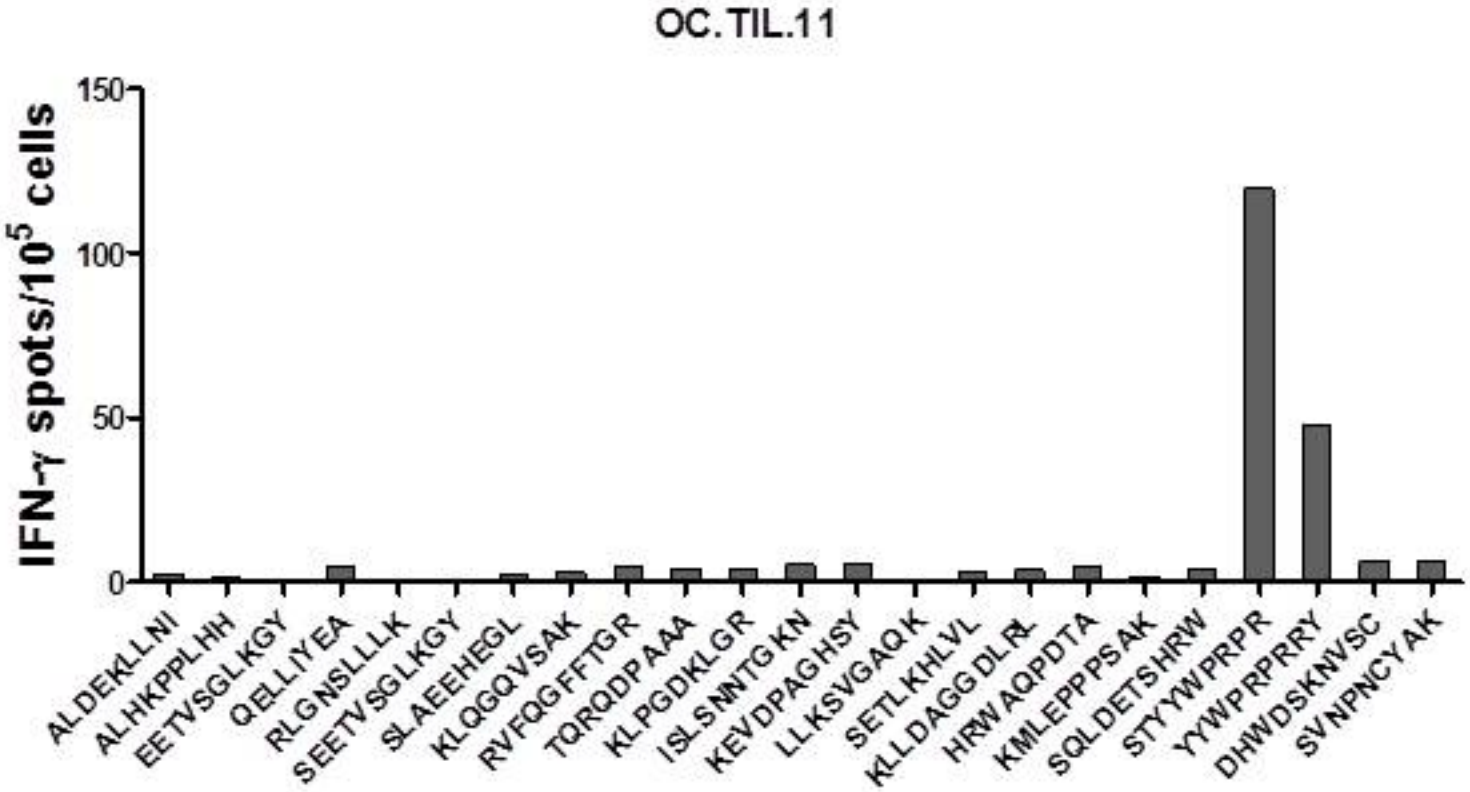
OC.TIL.11
IFN-γ spots/10^5 cells
150
100
50
0
ALDEKLLNI
ALHKPPLHH
EETVSGLKGY
QELLIYEA
RLGNSLLLK
SEETVSGLKGY
SLAEEHEGL
KLQGQVSAK
RVFQGFFTGR
TQRQDPAAA
KLPGDKLGR
ISLSNNTGKN
KEVDPAGHSY
LLKSVGAQK
SETLKHLVL
KLLDAGGDLRL
HRWAQPDTA
KMLEPPPSAK
SQLDETSHRW
STYYWPRPR
YYWPRPRRY
DHWDSKNVSC
SVNPNCYAK

B

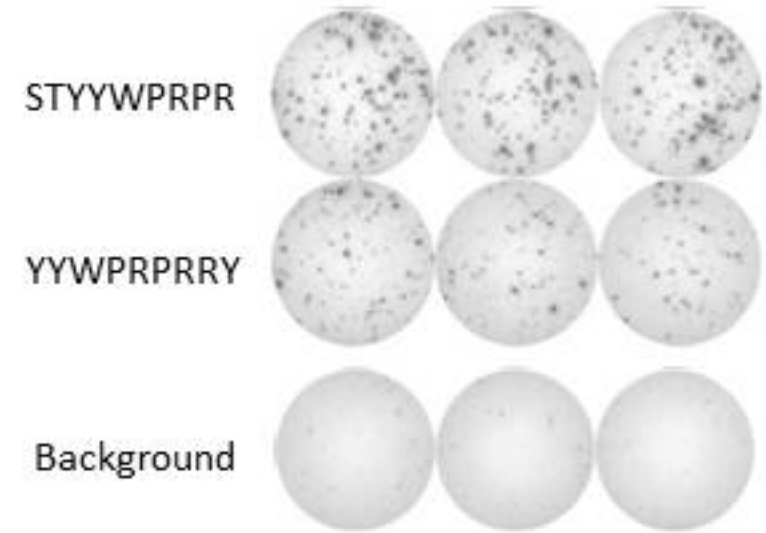
STYYWPRPR
YYWPRPRRY
Background

A

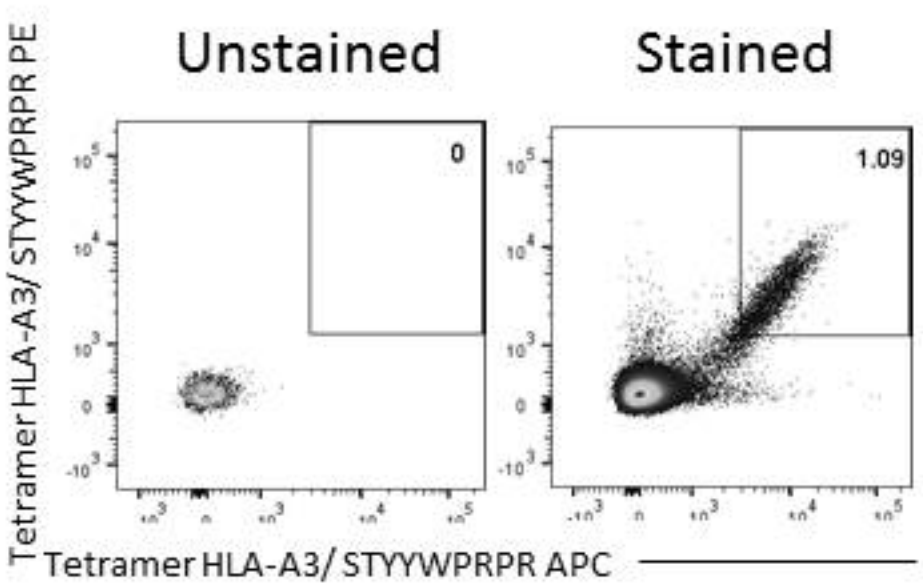
Unstained
Stained
0
1.09
Tetramer HLA-A3/ STYYWPRPR PE
Tetramer HLA-A3/ STYYWPRPR APC

B

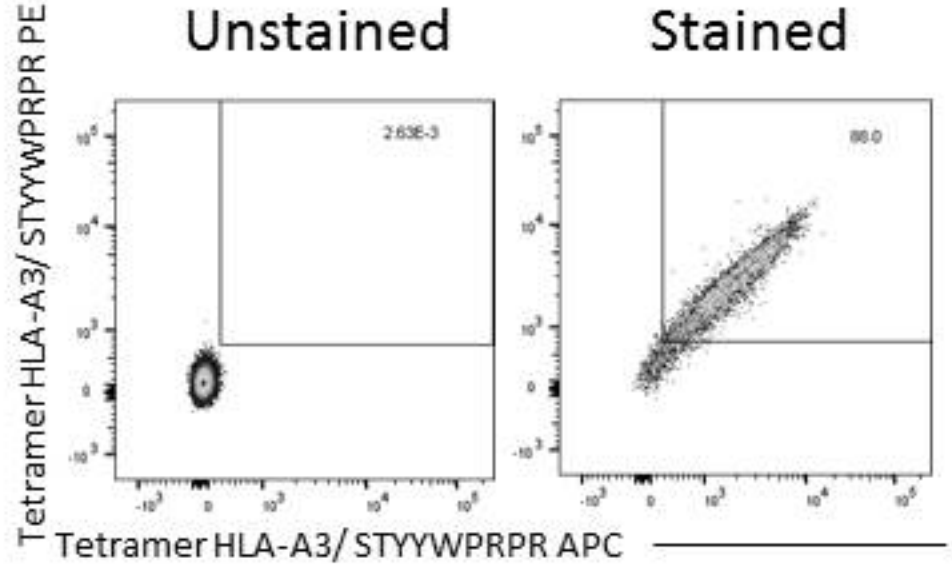
Unstained
Stained
2.63E-3
88.0
Tetramer HLA-A3/ STYYWPRPR PE
Tetramer HLA-A3/ STYYWPRPR APC

C

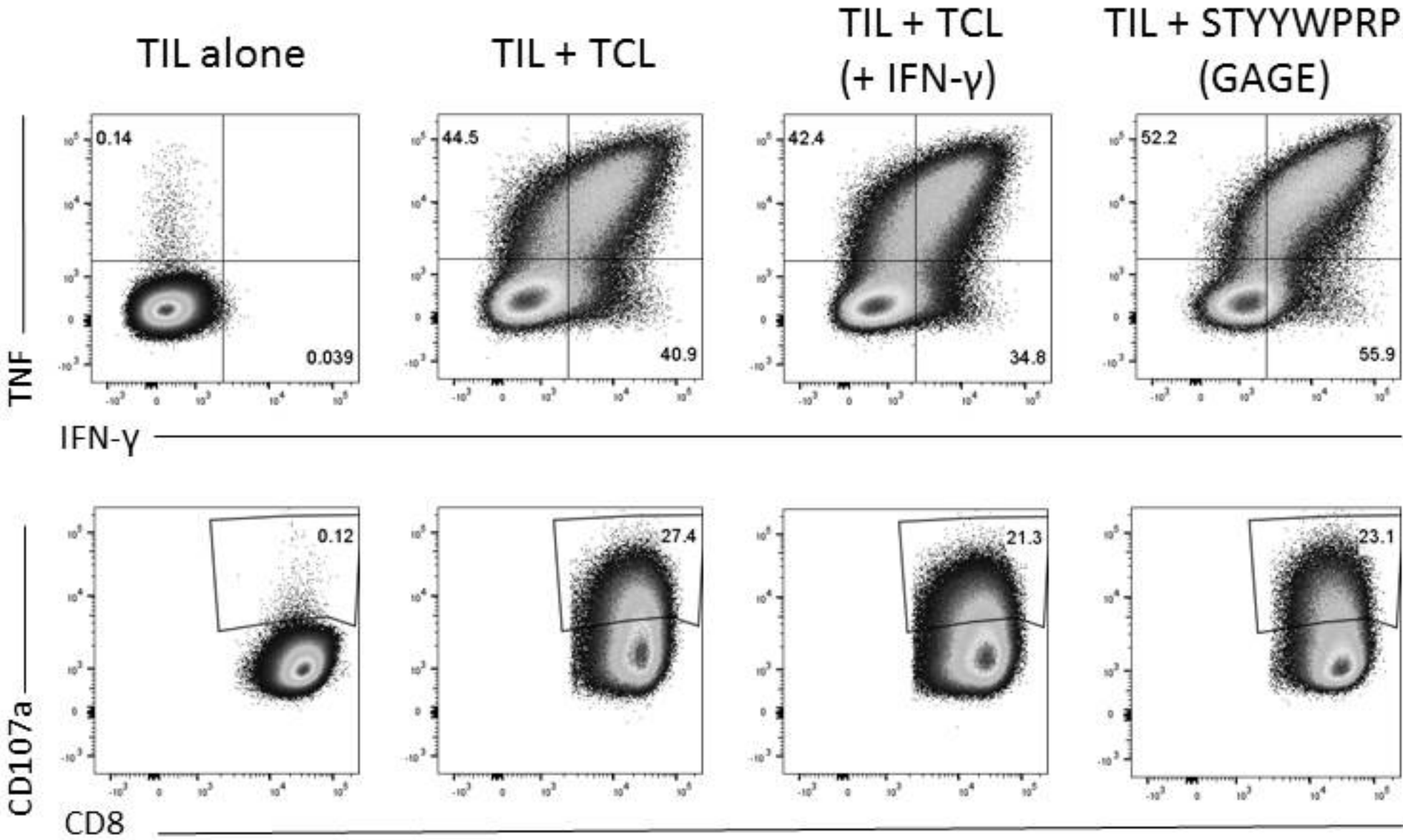
TIL alone
TIL + TCL
TIL + TCL (+ IFN-γ)
TIL + STYYWPRPR (GAGE)
0.14
0.039
44.5
40.9
42.4
34.8
52.2
55.9
TNF
IFN-γ
0.12
27.4
21.3
23.1
CD107a
CD8